MAP Symbol Detection of CPM Bursts

Peter A. Murphy, Gary E. Ford and Michael Golanbari
Department of Electrical and Computer Engineering
University of California, Davis, CA 95616
email: murphy@ece.ucdavis.edu, ford@ece.ucdavis.edu
golanbar@ece.ucdavis.edu
Tel: (916)752-0583

Abstract

A receiver is developed for MAP symbol detection of a burst (i.e., finite-length) CPM signal received in additive white Gaussian noise. This minimum probability of symbol error receiver requires the entire burst of data and involves the use of both forward and backward recursions. Performance results are provided comparing the MAP symbol detector to the more commonly used ML sequence detector (i.e., the Viterbi detector) applied to GMSK signals with the same burst structure as those employed in the GSM system. It is also shown that using only the forward recursions, the transmitted symbols can be detected in real-time (i.e., without the delay required by the ML sequence detector or the MAP symbol detector) with only slight degradation in performance.

1 Introduction

This section provides a brief introduction describing the importance of the problem of detection of burst continuous phase modulated (CPM) signals. We also introduce our approach for doing MAP symbol detection and provide a review of previous approaches to the general problem of MAP symbol detection.

1.1 Background & Goal

In digital communication systems, one of the most frequently used methods of separating users who share a common channel is by ensuring that each user transmits during a different time interval. This strategy, which is important for helping present and future networks keep pace with the ever-increasing demands being placed on them, is known as time-division multiple access (TDMA). Nowhere is the TDMA concept more useful than in mobile radio and personal communication systems (PCS) [1]. Time-division multiplexing different users' signals necessarily means that the sequence of symbols to be detected during each transmission period are burst sequences.

In this paper, we consider the transmission of such bursts and focus on developing minimum probability of symbol error receivers for the case when the symbols are transmitted using CPM signaling. CPM is an important modulation format because of its spectral efficiency and constant envelope, which allows for the use of nonlinear amplifiers [2]. Examples of systems that employ CPM signaling include the GSM cellular system [3,4], and the DCS1800 and DCS1900 PCS systems [5,6].

1.2 CPM Signal Model

We assume the burst structure is that of the GSM system [8], with a symbol burst of $N + 2L - 1$ bits, each drawn from the alphabet $\{-1, +1\}$. The first and last L bits are assumed known, and the remaining

N information bits are assumed independent and equally likely. Letting $\mathbf{b}$ denote this sequence of bits, we have

$$\mathbf{b} = [\underbrace{b_0, b_1, \cdots, b_{L-1}}_{\text{L known bits}}, \underbrace{b_L, b_{L+1}, \cdots, b_{N+L-1}}_{\text{N unknown bits}}, \underbrace{b_{N+L}, b_{N+L+1}, \cdots, b_{N+2L-1}}_{\text{L known bits}}]. \tag{1}$$

Using the Laurent representation [7] (see Appendix A), the complex baseband equivalent of the CPM signal generated from $\mathbf{b}$ can be expressed as

$$s(t, \mathbf{b}) = \sqrt{\frac{2E_b}{T}} \sum_{k=0}^{K-1} \sum_{n=0}^{N+2L-1} [e^{j\pi h a_{k,n}}] c_k(t - nT). \tag{2}$$

At the receiver we assume that the transmitted signal is distorted by noise, so that the received signal can be modeled as

$$r(t) = s(t, \mathbf{b}) + n(t), \tag{3}$$

where $n(t)$ is a realization of a zero-mean, circularly symmetric, white, Gaussian noise process with double-sided spectral density N_0.

1.3 The Approach

Optimal detection of CPM signals is accomplished by maximizing the probability of estimating the transmitted sequence correctly. Under the assumption that the transmitted symbols are independent and equally likely, this maximum a posteriori sequence detector (MAPSD) is equivalent to the maximum likelihood sequence detector (MLSD) [9], whose optimization criterion is

$$\hat{\mathbf{b}} = \arg \left\{ \max_{\mathbf{b}} [p(r(t)|\mathbf{b})] \right\}. \tag{4}$$

It is important to highlight that in the case of sequence detection, an error occurs when one or more of the symbols comprising $\hat{\mathbf{b}}$ does not equal the corresponding entry in $\mathbf{b}$.

Our approach is not based on optimum sequence detection, but rather on optimum symbol detection. The optimization criterion we are concerned with is

$$\hat{b}_n = \arg \left\{ \max_{b_n} [P(b_n|r(t))] \right\}, \ n \in [L, N + L - 1], \tag{5}$$

where b_n is one of the information bits comprising $\mathbf{b}$ in (1).

Using the Laurent representation, knowledge of the noise statistics, and the structure of $\mathbf{b}$, we show that (5) can be solved using a forward-backward recursive algorithm, which requires processing the entire burst of data before any one symbol estimate is available. We should point out that this forward-backward structure resembles the well-known solution for fixed-interval smoothing [10].

1.4 Related Work

In this section, we provide a review of previous approaches to the problem of minimum probability of symbol error detection. We begin by describing methods applied to CPM signaling and then describe techniques developed for ISI-corrupted PAM signals.

Osborne and Luntz [11] considered the development of minimum probability of symbol error receivers for CPFSK signals (i.e., CPM with 1REC pulses [2]) based upon a finite-length observation of the received signal. This fixed-delay constraint receiver makes decisions about one symbol based upon the present symbol interval and D signal intervals into the future. Once this decision is made, the receiver, in theory, starts from scratch to estimate the next symbol. In [12], Schonhoff extended the work of Osborne and Luntz to M-ary CPFSK signals. The main difference between these methods and our method is that in both [11] and [12], the MAP estimates are based upon a fixed-delay constraint, whereas we have no constraints other than the burst structure of the signal.

For ISI-corrupted PAM signals, a great deal of research has been done in developing MAP symbol detectors under a fixed-delay constraint [13–15]. It is shown in these references that the optimum receiver admits a forward-backward recursive structure. In the Appendix of [16], Forney provides a succinct outline of the forward and backward recursions required for MAP state detection for a finite-length, finite-state, discrete-time Markov process observed in memoryless noise. He goes on to illustrate how these estimates can be used to compute MAP symbol estimates for an ISI-corrupted PAM signal received in additive white Gaussian noise. Bahl et al. [17] developed results similar to that of Forney for MAP detection of linear block and convolutional codes. In [18], Verdu develops an MAP symbol detector for a multiple access channel shared by K asynchronous users. The MAP algorithm requires the entire received signal and involves forward and backward recursions.

1.5 Organization

The paper is organized as follows. In Section 2, we develop the MAP symbol detection algorithm. Section 3 provides performance results generated from computer simulations, comparing the MAP symbol detector to the more commonly used ML sequence detector. Finally, in Section 4, we provide some concluding remarks and issues to be researched in the future.

2 The Algorithm

In this section, we present the details of the the MAP symbol detection algorithm. In Section 2.1, we detail the MAP criterion and use our assumed knowledge of the noise statistics and the structure of the CPM burst to develop the optimum receiver. Following this, Section 2.2 includes the development of the forward and backward recursions, along with the initial conditions on these recursions. Lastly, Section 2.3 lists the main components of the algorithm and provides an outline of the steps necessary to do MAP symbol detection.

2.1 MAP Symbol Detection

Referring back to the signal model of Section 1.2, the received signal is given by

$$r(t) = s(t, \mathbf{b}) + n(t) \tag{6}$$

where $s(t, \mathbf{b})$ is given by (2) and $n(t)$ is a realization of a zero-mean, circularly symmetric white Gaussian noise process with double-sided spectral density N_0. We wish to develop the receiver structure that provides the MAP (i.e., the minimum probability of error) estimate of each element b_n of the sequence of transmitted symbols $\mathbf{b}$ given by (1). The MAP criterion for this estimate is

$$\hat{b}_n = \arg\left\{\max_{b_n} [P(b_n|r(t))]\right\}, \ n \in [L, N+L-1], \tag{7}$$

We will find it useful to define the state of the signal at time nT (see Appendix A) as

$$\mathbf{x}_n \triangleq [\theta_n, b_{n-L+1}, b_{n-L+2}, \cdots, b_{n-1}] \tag{8}$$

where

$$\theta_n = \pi h \sum_{i=0}^{n-L} b_i. \tag{9}$$

Assuming the modulation index $h = 2i/p$ (i, p integers), it can be shown that θ_n takes on p discrete values $\{0,\, 2\pi/p,\, \cdots,\, 2\pi(p-1)/p\}$. Using the definition of $\mathbf{x}_n$, we can express the conditional probability of (7) as

$$\begin{aligned} P(b_n|r(t)) &= \sum_{\theta_{n+1}} \sum_{b_{n-L+2}} \cdots \sum_{b_{n-1}} P(\theta_{n+1}, b_{n-L+2}, \cdots b_{n-1}, b_n|r(t)) && (10) \\ &= \sum_{\mathbf{x}_{n+1}=[\cdot,\cdots,b_n]} P(\mathbf{x}_{n+1}|r(t)). && (11) \end{aligned}$$

The MAP estimate of b_n can now be written as

$$\hat{b}_n = \arg\left\{\max_{b_n}\left[\sum_{\mathbf{x}_{n+1}=[\cdot,\cdots,b_n]} P(\mathbf{x}_{n+1}|r(t))\right]\right\}. \tag{12}$$

Considering the conditional density in (12) more closely, we write

$$\begin{aligned} P(\mathbf{x}_n|r(t)) &= \sum_{b_L}\cdots\sum_{b_{n-L}}\sum_{b_n}\cdots\sum_{b_{N+L-1}} P(b_L,\cdots,b_{n-L},\mathbf{x}_n,b_n,\cdots,b_{N+L-1}|r(t)) && (13)\\ &= \sum_{b_L}\cdots\sum_{b_{n-L}}\sum_{b_n}\cdots\sum_{b_{N+L-1}} p(r(t)|b_L,\cdots,b_{n-L},\mathbf{x}_n,b_n,\cdots,b_{N+L-1}) \\ &\quad\times\frac{P(b_L,\cdots,b_{n-L},\mathbf{x}_n,b_n,\cdots,b_{N+L-1})}{p(r(t))}. && (14)\end{aligned}$$

Since the term $p(r(t))$ has no effect on the maximization in (12), we let $d_1 = 1/p(r(t))$ and write

$$\begin{aligned} P(\mathbf{x}_n|r(t)) &= d_1\sum_{b_L}\cdots\sum_{b_{n-L}}\sum_{b_n}\cdots\sum_{b_{N+L-1}} p(r(t)|b_L,\cdots,b_{n-L},\mathbf{x}_n,b_n,\cdots,b_{N+L-1}) && (15)\\ &\quad\times P(b_L,\cdots,b_{n-L},\theta_n)\underbrace{P(b_{n-L+1},\cdots,b_{N+L-1})}_{\text{constant}} && (16)\\ &= d_2\sum_{b_L}\cdots\sum_{b_{n-L}}\sum_{b_n}\cdots\sum_{b_{N+L-1}} p(r(t)|b_L,\cdots,b_{n-L},\mathbf{x}_n,b_n,\cdots,b_{N+L-1}) \\ &\quad\times P(b_L,\cdots,b_{n-L},\theta_n), && (17)\end{aligned}$$

where $d_2 = d_1 P(b_{n-L+1},\cdots,b_{N+L-1})$ follows because the symbols are assumed independent and equally likely.

Using the Laurent representation (see Appendix A) and the fact that the noise is zero-mean, circularly symmetric and Gaussian with double-sided spectral density N_0, we can write

$$\begin{aligned} P(\mathbf{x}_n|r(t)) &= d_3\sum_{b_L}\cdots\sum_{b_{n-L}}\sum_{b_n}\cdots\sum_{b_{N+L-1}} \exp\left\{\frac{-1}{N_0}\int_{-\infty}^{\infty}\left|r(t)\right.\right. \\ &\quad\left.\left. -\sqrt{\frac{2E_b}{T}}\sum_{k=0}^{K-1}\sum_{l=0}^{N+2L-1} e^{j\pi h a_{k,l}} c_k(t-lT)\right|^2 dt\right\} P(b_L,\cdots,b_{n-L},\theta_n). && (18)\end{aligned}$$

Next, we let $y_{k,l}$ denote the output of the matched filter $c_k^*(-t)$ sampled at time $t = lT$ whose input is the received signal $r(t)$, i.e.,

$$y_{k,l} = \int_{-\infty}^{\infty} r(t)c_k^*(t-lT)dt. \tag{19}$$

Now define the vectors

$$\begin{aligned} \mathbf{e}_l &\triangleq [e^{j\pi h a_{0,l}}, e^{j\pi h a_{1,l}},\cdots,e^{j\pi h a_{K-1,l}}]^T && (20)\\ \mathbf{y}_l &\triangleq [y_{0,l},y_{1,l},\cdots,y_{K-1,l}]^T. && (21)\end{aligned}$$

This allows us to express (18) as

$$\begin{aligned} P(\mathbf{x}_n|r(t)) &= d_4\sum_{b_L}\cdots\sum_{b_{n-L}}\sum_{b_n}\cdots\sum_{b_{N+L-1}} \exp\left\{\frac{2}{N_0}\sqrt{\frac{2E_b}{T}}Re\sum_{l=0}^{N+2L-1}\mathbf{e}_l^H\mathbf{y}_l\right\} \\ &\quad\times P(b_L,\cdots,b_{n-L},\theta_n)\end{aligned}$$

$$\begin{aligned} &= d_4 \sum_{b_L} \cdots \sum_{b_{n-L}} \exp\left\{ \frac{2}{N_0}\sqrt{\frac{2E_b}{T}} Re \sum_{l=0}^{n-1} \mathbf{e}_l^H \mathbf{y}_l \right\} P(b_L, \cdots, b_{n-L}, \theta_n) \\ &\quad \times \sum_{b_n} \cdots \sum_{b_{N+L-1}} \exp\left\{ \frac{2}{N_0}\sqrt{\frac{2E_b}{T}} Re \sum_{l=n}^{N+2L-1} \mathbf{e}_l^H \mathbf{y}_l \right\} \\ &= d_4 F(\mathbf{x}_n) B(\mathbf{x}_n), \end{aligned} \tag{22}$$

where d_3 is a function of d_2 and N_0,

$$d_4 = d_3 \exp\left\{ \frac{-1}{N_0} \int_{-\infty}^{\infty} \left[|r(t)|^2 + 2E_b/T \right] dt \right\}, \tag{23}$$

and

$$F(\mathbf{x}_n) = \sum_{b_L} \cdots \sum_{b_{n-L}} \exp\left\{ \frac{2}{N_0}\sqrt{\frac{2E_b}{T}} Re \sum_{l=0}^{n-1} \mathbf{e}_l^H \mathbf{y}_l \right\} P(b_L, \cdots, b_{n-L}, \theta_n) \tag{24}$$

$$B(\mathbf{x}_n) = \sum_{b_n} \cdots \sum_{b_{N+L-1}} \exp\left\{ \frac{2}{N_0}\sqrt{\frac{2E_b}{T}} Re \sum_{l=n}^{N+2L-1} \mathbf{e}_l^H \mathbf{y}_l \right\}. \tag{25}$$

In the next section, we will demonstrate that $F(\mathbf{x}_n)$ and $B(\mathbf{x}_n)$ can be calculated using forward and backward recursions, respectively. However, before doing so, it is interesting to note that $F(\mathbf{x}_n)$ can be thought of as the probability of being in state $\mathbf{x}_n$ given $r(t)$ for $t \leq (n+L)T$, i.e.,

$$F(\mathbf{x}_n) \approx P(\mathbf{x}_n | r(t), t \leq (n+L)T). \tag{26}$$

Similarly, $B(\mathbf{x}_n)$ can be thought of as the probability of being in state $\mathbf{x}_n$ given $r(t)$ for $t \geq nT$, i.e.,

$$B(\mathbf{x}_n) \approx P(\mathbf{x}_n | r(t), t \geq nT). \tag{27}$$

2.2 The Forward and Backward Recursions

Based upon (9) and the fact that the modulation index is assumed to be expressible as $h = 2i/p$ (i, p integers), it can be shown that

$$P(b_L, \cdots, b_{n-L}, \theta_n) = \sum_{\theta_{n-1}} P(b_L, \cdots, b_{n-L-1}, \theta_{n-1}) P(b_{n-L}) P(\theta_{n-1}, b_{n-L} | \theta_n). \tag{28}$$

This allows us to write (24) as

$$\begin{aligned} F(\mathbf{x}_n) &= \sum_{\mathbf{x}_{n-1}} \sum_{b_L} \cdots \sum_{b_{n-L-1}} \exp\left\{ \frac{2}{N_0}\sqrt{\frac{2E_b}{T}} Re \sum_{l=0}^{n-1} \mathbf{e}_l^H \mathbf{y}_l \right\} P(b_L, \cdots, b_{n-L-1}, \theta_{n-1}) \\ &\quad \times P(b_{n-L}) P(\mathbf{x}_{n-1} | \mathbf{x}_n) \\ &= \sum_{\mathbf{x}_{n-1}} \sum_{b_L} \cdots \sum_{b_{n-L-1}} \exp\left\{ \frac{2}{N_0}\sqrt{\frac{2E_b}{T}} Re \sum_{l=0}^{n-2} \mathbf{e}_l^H \mathbf{y}_l \right\} P(b_L, \cdots, b_{n-L-1}, \theta_{n-1}) \\ &\quad P(\mathbf{x}_{n-1} | \mathbf{x}_n) \exp\left\{ \frac{2}{N_0}\sqrt{\frac{2E_b}{T}} Re \left(\mathbf{e}_{n-1}^H \mathbf{y}_{n-1} \right) \right\} P(b_{n-L}) \\ &= \sum_{\mathbf{x}_{n-1}} F(\mathbf{x}_{n-1}) P(\mathbf{x}_{n-1} | \mathbf{x}_n) G_F(\mathbf{x}_{n-1}, \mathbf{x}_n), \end{aligned} \tag{29}$$

where

$$G_F(\mathbf{x}_{n-1}, \mathbf{x}_n) = \exp\left\{ \frac{2}{N_0}\sqrt{\frac{2E_b}{T}} Re\left(\mathbf{e}_{n-1}^H \mathbf{y}_{n-1}\right)\right\} P(b_{n-L}) \tag{30}$$

$$= \frac{1}{2}\exp\left\{ \frac{2}{N_0}\sqrt{\frac{2E_b}{T}} Re\left(\mathbf{e}_{n-1}^H \mathbf{y}_{n-1}\right)\right\}. \tag{31}$$

Equation (31) follows from (30) because the symbols are assumed independent and equally likely.

Next, we develop the backwards recursions for calculating $B(\mathbf{x}_n)$. From (25), we write

$$\begin{aligned} B(\mathbf{x}_n) &= \sum_{b_n}\cdots\sum_{b_{N+L-1}} \exp\left\{ \frac{2}{N_0}\sqrt{\frac{2E_b}{T}} Re \sum_{l=n}^{N+2L-1} \mathbf{e}_l^H \mathbf{y}_l \right\} \\ &= c_4 \sum_{\mathbf{x}_{n+1}} \sum_{b_{n+1}} \cdots \sum_{b_{N+L-1}} \exp\left\{ \frac{2}{N_0}\sqrt{\frac{2E_b}{T}} Re \sum_{l=n}^{N+2L-1} \mathbf{e}_l^H \mathbf{y}_l \right\} P(\mathbf{x}_{n+1}|\mathbf{x}_n) \\ &= c_4 \sum_{\mathbf{x}_{n+1}} \sum_{b_{n+1}} \cdots \sum_{b_{N+L-1}} \exp\left\{ \frac{2}{N_0}\sqrt{\frac{2E_b}{T}} Re \sum_{l=n+1}^{N+2L-1} \mathbf{e}_l^H \mathbf{y}_l \right\} P(\mathbf{x}_{n+1}|\mathbf{x}_n) \\ &\quad \times \exp\left\{ \frac{2}{N_0}\sqrt{\frac{2E_b}{T}} Re\left(\mathbf{e}_n^H \mathbf{y}_n\right)\right\} \\ &= c_4 \sum_{\mathbf{x}_{n+1}} B(\mathbf{x}_{n+1}) P(\mathbf{x}_{n+1}|\mathbf{x}_n) G_B(\mathbf{x}_n, \mathbf{x}_{n+1}), \end{aligned} \tag{32}$$

where c_4 is a constant equal to $1/P(b_n)$ and

$$G_B(\mathbf{x}_n, \mathbf{x}_{n+1}) = \exp\left\{ \frac{2}{N_0}\sqrt{\frac{2E_b}{T}} Re\left(\mathbf{e}_n^H \mathbf{y}_n\right)\right\}. \tag{33}$$

Next, we determine the initial conditions on the forward and backward recursions. From (1), we see that our goal is to calculate $\hat{b}_n$ using (12) for $n \in [L, N+L-1]$. Equation (22) reveals that estimation of these symbols requires calculating $F(\mathbf{x}_n)$ and $B(\mathbf{x}_n)$ for $n \in [L+1, N+L]$. Based upon these results, it can be shown that the initial conditions on the forward recursions are given by

$$F(\mathbf{x}_L) = \begin{cases} 1, & \mathbf{x}_L = [\pi h b_0, b_1, \cdots, b_{L-1}] \\ 0, & \mathbf{x}_L \neq [\pi h b_0, b_1, \cdots, b_{L-1}] \end{cases} \tag{34}$$

Calculating the initial conditions for the backward recursions is more complex. In order to simplify things we consider the case in which the modulation index $h = 1/2$. (Note that in the simulation results presented in Section 3, we choose $h = 1/2$ and $L = 3$.) Under these assumptions, it can be shown that

$$B(\mathbf{x}_{N+2L-1}) = \begin{cases} 1/2, & \mathbf{x}_{N+2L-1} = [0 \text{ or } \pi, b_{N+L}, \cdots, b_{N+2L-2}],\ N+2L-1 \text{ even} \\ 0, & \mathbf{x}_{N+2L-1} \neq [0 \text{ or } \pi, b_{N+L}, \cdots, b_{N+2L-2}],\ N+2L-1 \text{ even} \\ & \\ 1/2, & \mathbf{x}_{N+2L-1} = [\pi/2 \text{ or } 3\pi/2, b_{N+L}, \cdots, b_{N+2L-2}],\ N+2L-1 \text{ odd} \\ 0, & \mathbf{x}_{N+2L-1} \neq [\pi/2 \text{ or } 3\pi/2, b_{N+L}, \cdots, b_{N+2L-2}],\ N+2L-1 \text{ odd} \end{cases} \tag{35}$$

2.3 Algorithm Review

In the following, we provide a review of the main components of the MAP symbol detection algorithm presented in Sections 2.1 and 2.2.

Assumptions:

1. The information bits are independent and equally likely, with the transmitted sequence given by

$$\mathbf{b} = [\underbrace{b_0, b_1, \cdots, b_{L-1}}_{\text{L known bits}}, \underbrace{b_L, b_{L+1}, \cdots, b_{N+L-1}}_{\text{N unknown bits}}, \underbrace{b_{N+L}, b_{N+L+1}, \cdots, b_{N+2L-1}}_{\text{L known bits}}]. \quad (36)$$

2. The state is defined as

$$\mathbf{x}_n \triangleq [\theta_n, b_{n-L+1}, b_{n-L+2}, \cdots, b_{n-1}]. \quad (37)$$

3. The phase state is given by

$$\theta_n = \pi h \sum_{i=0}^{n-L} b_i. \quad (38)$$

<u>MAP Symbol Detection:</u>

$$\hat{b}_n = \arg\left\{\max_{b_n}\left[\sum_{\mathbf{x}_{n+1}=[\cdot,\cdots,b_n]} P(\mathbf{x}_{n+1}|r(t))\right]\right\} \quad (39)$$

$$P(\mathbf{x}_n|r(t)) = d_4 F(\mathbf{x}_n) B(\mathbf{x}_n) \quad (40)$$

$$F(\mathbf{x}_n) = \sum_{\mathbf{x}_{n-1}} F(\mathbf{x}_{n-1}) P(\mathbf{x}_{n-1}|\mathbf{x}_n) G_F(\mathbf{x}_{n-1}, \mathbf{x}_n) \quad (41)$$

$$B(\mathbf{x}_n) = c_4 \sum_{\mathbf{x}_{n+1}} B(\mathbf{x}_{n+1}) P(\mathbf{x}_{n+1}|\mathbf{x}_n) G_B(\mathbf{x}_n, \mathbf{x}_{n+1}) \quad (42)$$

$$G_F(\mathbf{x}_{n-1}, \mathbf{x}_n) = \frac{1}{2}\exp\left\{\frac{2}{N_0}\sqrt{\frac{2E_b}{T}} Re\left(\mathbf{e}_{n-1}^H \mathbf{y}_{n-1}\right)\right\} \quad (43)$$

$$G_B(\mathbf{x}_n, \mathbf{x}_{n+1}) = \exp\left\{\frac{2}{N_0}\sqrt{\frac{2E_b}{T}} Re\left(\mathbf{e}_n^H \mathbf{y}_n\right)\right\} \quad (44)$$

$$\mathbf{e}_l \triangleq [e^{j\pi h a_{0,l}}, e^{j\pi h a_{1,l}}, \cdots, e^{j\pi h a_{K-1,l}}]^T \quad (45)$$

$$\mathbf{y}_l \triangleq [y_{0,l}, y_{1,l}, \cdots, y_{K-1,l}]^T \quad (46)$$

$$y_{k,l} = \int_{-\infty}^{\infty} r(t) c_k^*(t - lT) dt \quad (47)$$

<u>The Constants:</u>

$$d_1 = 1/p(r(t)) \quad (48)$$

$$d_2 = d_1 P(b_{n-L+1}, \cdots, b_{N+L-1}) \quad (49)$$

$$d_3 = f(d_2, N_0) \quad (50)$$

$$d_4 = d_3 \exp\left\{\frac{-1}{N_0}\int_{-\infty}^{\infty}\left[|r(t)|^2 + 2E_b/T\right] dt\right\} \quad (51)$$

The constants in equations (40), (42), and (43) can be set equal to 1 with no loss in performance. This is because their presence in (39) does not effect the choice of $\hat{b}_n$.

<u>Initial Conditions:</u>

$$F(\mathbf{x}_L) = \begin{cases} 1, & \mathbf{x}_L = [\pi h b_0, b_1, \cdots, b_{L-1}] \\ 0, & \mathbf{x}_L \neq [\pi h b_0, b_1, \cdots, b_{L-1}] \end{cases} \quad (52)$$

$$B(\mathbf{x}_{N+2L-1}) = \begin{cases} 1/2, & \mathbf{x}_{N+2L-1} = [0 \text{ or } \pi, b_{N+L}, \cdots, b_{N+2L-2}],\ N+2L-1 \text{ even} \\ 0, & \mathbf{x}_{N+2L-1} \neq [0 \text{ or } \pi, b_{N+L}, \cdots, b_{N+2L-2}],\ N+2L-1 \text{ even} \\ & \\ 1/2, & \mathbf{x}_{N+2L-1} = [\pi/2 \text{ or } 3\pi/2, b_{N+L}, \cdots, b_{N+2L-2}],\ N+2L-1 \text{ odd} \\ 0, & \mathbf{x}_{N+2L-1} \neq [\pi/2 \text{ or } 3\pi/2, b_{N+L}, \cdots, b_{N+2L-2}],\ N+2L-1 \text{ odd} \end{cases} \quad (53)$$

Note the initial conditions on the backward recursions are for the specific case when $h = 1/2$.

3 Performance

In this section, we present performance results for the MAP symbol detection algorithm introduced in Section 2. These computer simulations were done in the MATLAB 4.2c environment. The CPM signals were modeled after the GMSK signals used in the GSM cellular system. More specifically, the GMSK signal parameters are $BT = 0.3$, $L = 3$ and $h = 1/2$. We also chose the length of each burst $N + 2L - 1$ to be equal to the bursts used in the GSM system (i.e., N=156). All processing was done at complex baseband.

Figure 1 is a plot of the BER vs E_b/N_o characteristics for the MAP symbol detector developed in this paper and the ML sequence detector developed in [19]. This plot provides the interesting result that both detectors perform the same (except for $E_b/N_o = 8\,dB$, but we attribute this to computational limitations). This suggests that for CPM signals, the ML sequence detector provides the same symbol estimates as the MAP symbol detector, and, therefore, minimizes the probability of making a symbol error. Or said in a different way, the ML sequence detector, which can be thought of as globally optimum, is also locally optimum, like the MAP symbol detector.

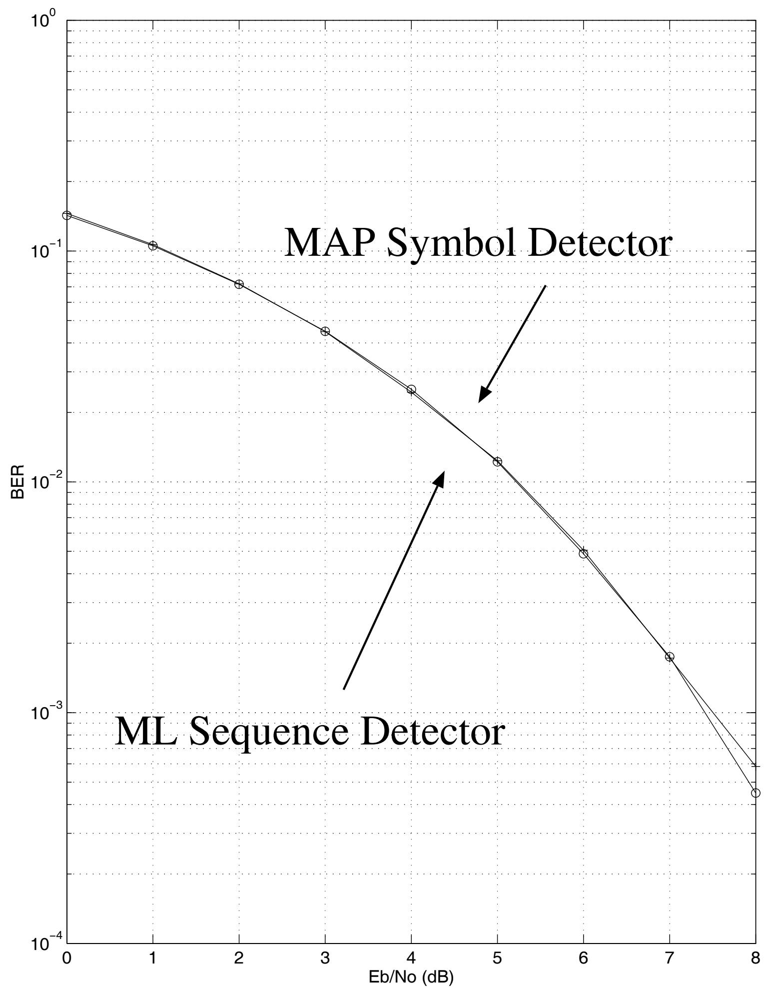

Figure 1: MAP symbol detector vs. ML sequence detector, N=156.

It was of interest to us to determine how important the individual contributions from the forward and backward recursions are in providing the MAP symbol estimate. Therefore, as a test we considered comparing the performance of the optimum MAP symbol detector, which uses both the forward and backward recursions, to the detector which only considers the forward recursions (i.e, set $B(\mathbf{x}_n) = 1$ in (40)). The results are presented in Figure 2. The plot reveals that as we had suspected, the backward recursions provide very little information about the probability of being in state $\mathbf{x}_n$ and that nearly all the processing power of the algorithm resides in the forward recursions. This result actually is not surprising if one considers

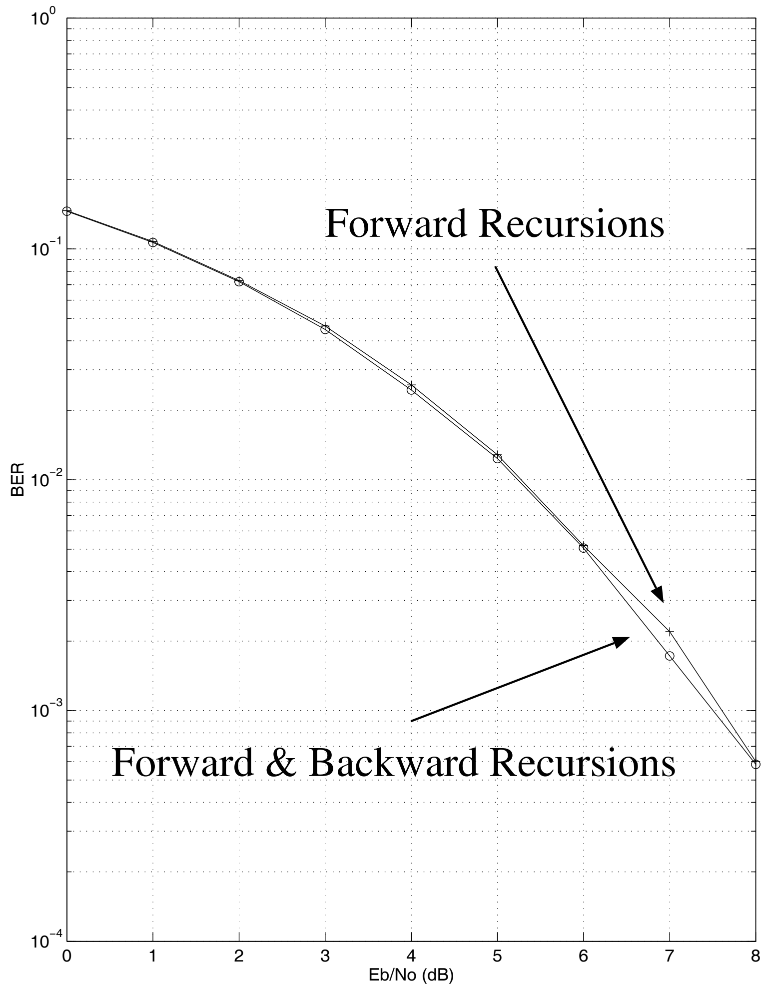

Figure 2: MAP symbol detector comparing forward-backward to forward, N=156.

that during the calculation of the backward recursions in going from state $\mathbf{x}_{n+1}$ to $\mathbf{x}_n$, for the specific case of $L = 3$, it is the symbol b_{n-2} that provides the transition between states. Looking more closely at the Laurent representation (2), it can be shown that for $t = nT$, b_{n-2} only affects the complex exponentials $e^{j\pi h a_{2,n}}$ and $e^{j\pi h a_{3,n}}$ multiplying the two smallest pulses $c_2(t - nT)$ and $c_3(t - nT)$. Note that it has been shown [19] that these two components contain less than 1% of the CPM signal power. Therefore, when calculating the metric given in (44), which is a function of the matched filter outputs $\mathbf{y}_n$, there will be very little difference for the cases $b_{n-2} = +1$ and $b_{n-2} = -1$. This is the reason why the backward recursions provide so little information.

What is interesting to realize is that if the backward recursions are expendable, then we can simply detect the symbols based upon the forward recursions, with these estimates being nearly optimum. Recall that at the end of Section 2.1, we noted that $F(\mathbf{x}_n)$ can be thought of as the probability of being in state $\mathbf{x}_n$ given $r(t)$ for $t \leq (n + L)T$. This result highlights that symbol estimates based upon $F(\mathbf{x}_n)$ (and not $B(\mathbf{x}_n)$) do not require that the entire burst of data be processed, but rather that we only have a processing delay of LT seconds before an estimate is available. This is certainly an advantage over the optimum MAP symbol detection algorithm (using both the forward and backward recursions) and the optimum ML sequence detection algorithm, which requires that the entire burst of data be received before any estimates are available.

4 Conclusions & Future Work

In this paper, we considered the transmission of a burst of symbols transmitted using CPM signaling. A receiver algorithm was developed that minimized the probability of symbol error under the assumption that the noise is white and Gaussian. We illustrated that this algorithm requires the use of both forward and backward recursions, and that the entire burst of data is required before any estimates are available. Performance results were presented which suggest the following:

- For the particular CPM signals considered, the MAP symbol detector developed here and the more commonly used ML sequence detector perform the same.
- Because of the structure of CPM signals, the backward recursions provide very little of the processing power of the MAP algorithm.
- It is the forward recursions which provide the information needed. For this reason, a nearly optimum receiver can be developed based solely on the forward recursions. The advantage of such a receiver is that only a delay of LT seconds is required before symbol estimates are available. This is in stark contrast to the MAP symbol detector and the ML sequence detectors, which require the entire burst of data before any estimates are available.

In the future we plan to consider the development of near-optimum symbol detectors based on the Laurent approximation, which uses only the $k = 0$ term in (2), in representing the CPM signal. This approach has proven to be quite useful in developing reduced-complexity sequence detectors for CPM signals [19]. We also plan to consider the development of an optimum symbol detector for the case when the symbols comprising the sequence $\mathbf{b}$ are not independent and equally likely, but are correlated due to precoding. Lastly, we will develop a complexity comparison between the MAP symbol detector and the ML sequence detector.

A The Laurent Representation

Consider the transmission of the sequence $\mathbf{b}$ given by (1). From [2], we know that the complex baseband CPM signal can be expressed as

$$s(t, \mathbf{b}) = \sqrt{\frac{2E_b}{T}} e^{j[\theta(t)]}, \quad t \geq 0 \tag{54}$$

$$\theta(t) = 2\pi h \int_0^t \sum_{i=0}^{N+2L-1} b_i g(\tau - iT) d\tau, \quad t \geq 0 \tag{55}$$

$$= \pi h \sum_{i=0}^{N+2L-1} b_i q(t - iT), \quad t \geq 0, \tag{56}$$

where E_b is the energy per bit, T is the bit period, h is the modulation index which takes on rational values (i.e., $h = 2k/p$ k, p integers), $\{b_i\}$ are the transmitted bits taken from the set $\{-1, 1\}$ with equal probability, $g(t)$ is termed the frequency pulse which is nonzero in the interval $[0, LT]$, has area equal to $1/2$ and is symmetric about $LT/2$, and $q(t)$ is the integral of the frequency pulse, such that

$$q(t) = \int_0^t g(\tau) d\tau \tag{57}$$

$$q(LT) = 1/2. \tag{58}$$

Laurent [7] showed that the complex baseband signal $s(t, \mathbf{b})$ can be expressed as the sum of $K = 2^{L-1}$ PAM signals, i.e.,

$$s(t, \mathbf{b}) = \sqrt{\frac{2E_b}{T}} \sum_{k=0}^{K-1} \sum_{n=0}^{N+2L-1} [e^{j\pi h a_{k,n}}] c_k(t - nT) \tag{59}$$

over the interval $t \in [LT, (N + 2L)T]$, where

$$\begin{aligned} a_{k,n} &= \sum_{i=o}^{n} b_i - \sum_{j=1}^{L-1} b_{n-j}\beta_{k,j} \\ &= a_{o,n} - \sum_{j=1}^{L-1} b_{n-j}\beta_{k,j}, \\ &= a_{o,n-L} + \sum_{j=1}^{L-1} b_{n-j}(1 - \beta_{k,j}) + b_n, \end{aligned} \tag{60}$$

where the set $\{\beta_{k,j}\}$ are used in the binary representation of the index k, i.e.,

$$k = \sum_{j=1}^{L-1} 2^{j-1}\beta_{k,j} \quad k \in [0, K-1] \tag{61}$$

and $\beta_{k,j} \in \{0, 1\}$.

Defining the state of the signal at time nT as

$$\mathbf{x}_n \triangleq [\theta_n, b_{n-L+1}, b_{n-L+2}, \cdots, b_{n-1}], \tag{62}$$

where

$$\theta_n = \pi h \sum_{i=0}^{n-L} b_i, \tag{63}$$

it can be shown that $e^{j\pi h a_{k,n}}$ in (59) is a function of the state $\mathbf{x}_n$ and the symbol b_n. Furthermore, for $h = 2i/p$ (i, p integers), it can be shown that θ_n takes on p discrete values $\{0, 2\pi/p, \cdots, 2\pi(p-1)/p\}$.

The functions of time $c_k(t)$ are given by

$$c_k(t) = s_0(t) \prod_{j=1}^{L-1} s_{j+L\beta k,j}(t) \quad k \in [0, K-1], \tag{64}$$

where

$$s_j(t) = \frac{sin(\Psi(t + jT))}{sin(\pi h)} = s_0(t + jT), \tag{65}$$

$$\Psi(t) = \begin{cases} \phi(t) & t \in [0, LT) \\ \pi h - \phi(t - LT) & t \in [LT, 2LT] \\ 0 & else \end{cases}$$

and

$$\phi(t) = 2\pi h \int_0^t g(\tau) d\tau. \tag{66}$$

References

[1] D. D. Falconer, F. Adachi, and B. Gudmundson, "Time division multiple access methods for wireless personal communications," *IEEE Communications Magazine*, pp. 50–57, Jan. 1995.

[2] J. Anderson, T. Aulin, and C. Sundberg, *Digital Phase Modulation.* New York, NY: Plenum Press, 1986.

[3] R. Steele, *Mobile Radio Communications.* London: Pentech, 1992.

[4] M. Hodges, "The GSM radio interface," *British Telecom Technology Journal*, vol. 8, no. 1, pp. 31 – 43, Jan. 1990.

[5] P. Ramsdale, "Personal communications in the UK – implementation of PCN using DCS 1800," *Internat. J. Wireless Info. Networks*, vol. 1, no. 1, pp. 29 – 36, Jan. 1994.

[6] J. E. Padgett, C. G. Gunther, and T. Hattori, "Overview of wireless personal communications," *IEEE Communications Magazine*, pp. 28 – 41, Jan. 1995.

[7] P. A. Laurent, "Exact and approximate construction of digital phase modulations by superposition of amplitude modulated pulses (AMP)," *IEEE Trans. Comm.*, vol. 34, no. 2, pp. 150 – 160, Feb. 1986.

[8] S. M. Redl, M. K. Weber, and M. W. Oliphant, *An Introduction To GSM.* Boston · London: Artech House, 1995.

[9] J. Proakis, *Digital Communications.* New York: McGraw–Hill, 1989.

[10] B. D. O. Anderson and J. B. Moore, *Optimal Filtering.* Englewood Cliffs, N.J.: Prentice-Hall, 1979.

[11] W. P. Osborne and M. B. Luntz, "Coherent and noncoherent detection of CPFSK," *IEEE Trans. Comm.*, vol. COM-22, no. 8, pp. 1023 – 1036, Aug. 1974.

[12] T. A. Schonhoff, "Symbol error probabilities for M-ary CPFSK: Coherent and noncoherent detection," *IEEE Trans. Comm.*, vol. COM-24, no. 6, pp. 644 – 652, June 1976.

[13] K. Abend, J. T. J. Hartley, B. D. Fritchman, and C. Gumacos, "On optimum receivers for channels having memory," *IEEE Trans. Inform. Theory*, vol. IT-14, pp. 819 – 820, Nov. 1968.

[14] R. R. Bowen, "Bayesian decision procedure for interfering digital signals," *IEEE Trans. Inform. Theory*, vol. IT-15, pp. 506 – 507, July 1969.

[15] K. Abend and B. D. Fritchman, "Statistical detection for communication channels with intersymbol interference," *Proc. IEEE*, vol. 58, no. 5, pp. 779 – 785, May 1970.

[16] G. D. Forney, "The Viterbi algorithm," *IEEE Proc.*, vol. 61, no. 3, pp. 268–278, Mar. 1973.

[17] L. R. Bahl, J. Cocke, F. Jelinek, and J. Raviv, "Optimal decoding of linear codes for minimizing symbol error rate," *IEEE Trans. Inform. Theory*, vol. IT-20, no. 2, pp. 284 – 287, Mar. 1974.

[18] S. Verdu, "On fixed-interval minimum symbol error probability detection," Tech. Rep. R-990, UILU ENG 83-2211, Coordinated Science Laboratory- University of Illinois at Urbana-Champaign, 1983.

[19] P. A. Murphy and G. E. Ford, "Joint demodulation of continuous phase modulated signals using the Laurent representation," in *Proceedings of 1996 Virginia Tech Symposium on Wireless Personal Communications*, (Blacksburg, VA), pp. 11–1 – 11–12, June 1996.